

# Dynamical effects in proton breakup from exotic nuclei

Ravinder Kumar<sup>a,b</sup> and Angela Bonaccorso<sup>a</sup>

<sup>a</sup>INFN, Sez. di Pisa and <sup>b</sup>Dipartimento di Fisica, Università di Pisa,  
Largo Pontecorvo 3, 56127 Pisa, Italy.

We study dynamical effects in proton breakup from a weakly bound state in an exotic nucleus on a heavy target. The Coulomb interactions between the proton and the core and the proton and the target are treated to all orders, including also the full multipole expansion of the Coulomb potential. The dynamics of proton nuclear and Coulomb breakup is compared to that of an *equivalent* neutron of larger binding energy in order to elucidate the differences with the well understood neutron breakup mechanism. A number of experimentally measurable observables such as parallel momentum distributions, proton angular distributions and total breakup cross sections are calculated. With respect to nuclear breakup it is found that a proton behaves exactly as a neutron of larger binding energy. The extra "effective energy" is due to the combined core-target Coulomb barrier. In Coulomb breakup we distinguish the effect of the core-target Coulomb potential (called recoil effect), with respect to which the proton behaves again as a more bound neutron, from the direct proton-target Coulomb potential. The latter gives cross sections about an order of magnitude larger than the recoil term. The two effects give rise to complicated interferences in the parallel momentum distributions. They are instead easily separable in the proton angular distributions which are therefore suggested as a very useful observable for future experimental studies.

**Pacs** 21.10.Jx, 24.10.-i, 25.60.Gc, 27.30.+t

## I. INTRODUCTION

In a recent paper Liang et al.[1] studied experimentally dynamical effects in the Coulomb breakup of  $^{17}\text{F}$ . The motivation was that Coulomb dissociation, being the inverse of the radiative capture reaction, is a useful technique for studying stellar nucleosynthesis involving short-lived nuclei where direct measurements are difficult [2]. The authors argued that with an increasing number of radioactive isotope beams available for studying capture reactions that occur in stellar environments, such as those in the rp-process, more measurements will be performed by Coulomb dissociation because of the short lifetimes that make direct measurements impractical. In order to extract reliable information on radiative capture the reaction mechanism in Coulomb dissociation has to be understood in detail. Furthermore Liang et al.[1] stressed the importance of the dynamic polarization effect which they interpret as a displacement of the valence proton behind the nuclear core and a subsequent shielding from the target. This effect manifests itself as a reduction of breakup probability compared to first-order perturbation theory predictions. Coulomb dissociation experiments [3]-[5] have been studied with different approaches, among which first-order perturbation theory is indeed often used with final plane wave functions. While Coulomb dissociation of loosely bound neutron-rich nuclei has been studied extensively and is fairly well understood [6, 7], this is not true for proton-rich nuclei in which the loosely bound valence protons actively participate in the reaction. It has also been suggested that the inclusion of higher-order corrections is required [8, 9]. Essentially exact calculations of realistic three-body models of break-up based on the Faddeev equations including the Coulomb potential exist for few body nuclei [10]. These methods have also been applied to neutron break up from medium mass exotic nuclei using cluster models [11] and it is expected that they should perform equally well for proton breakup.

Besides the well known astrophysical implications proton rich nuclei present a number of unusual features such as the two proton radioactivity or beta-delayed proton emission which make them very appealing to study and to compare to the neutron rich nuclei. An account of the richness of the "Physics of the proton rich side of the nuclear chart" can be found in Ref.[12].

In Ref.[1]  $^{17}\text{F} + ^{58}\text{Ni}$  and  $^{17}\text{F} + ^{208}\text{Pb}$  breakup angular distributions measured at 10A.MeV were discussed and compared to first-order perturbation theory prediction for Coulomb breakup and to fully dynamical calculations. At the end of their paper the authors used first-order perturbation theory to calculate proton breakup via an increase of the effective binding energy of the valence proton treated as if it were a neutron, according to a model that was proposed some time ago by some of us [13]. Liang et al. [1] found that our idea did indeed work and the angular distributions could successfully be reproduced using an increase in the binding energy of 1.2 MeV, contrary to our model suggestion of 3.2 MeV.

We were intrigued and interested by such a result: first we were happy to notice that our very schematic model would work in comparison with real data; second we decided that it was worth studying if and how the model could be made more quantitatively reliable. This paper reports results of such a study for some observables such as parallel

momentum distribution and proton angular distributions following breakup. A forthcoming paper will discuss core angular distributions.

In the next section we recall the model for nuclear and Coulomb breakup for a valence nucleon treated to all orders introduced in [14], that we developed successively in Ref.[15] to treat protons. Our starting point is, as in all our previous works, a first order perturbation theory amplitude such as that given by Eq.(1) of [16]. In that paper the amplitude was used for transfer to bound states, thus the neutron-target potential acted only to first order. On the other hand when the same formula is used for transitions to final unbound states [17], in order to describe breakup, the final state is a proper scattering state with respect to the target and thus all re-scattering terms are included [19, 20]. We then compare in Sec.III results of the full calculation to those of perturbation theory. The amount and characteristics of the breakup due to the core-target and to the proton-target Coulomb repulsions are then studied separately. We do that at fixed impact parameter values in order to understand the reduction of breakup probability for protons as compared to that of neutrons of the same binding. This is because our model predicted that the effective binding energy would depend on the distance between the two nuclei, being due to the mutual projectile-target Coulomb barrier. The impact parameter dependence enters also in the model of Ref. [15] where we showed that the Coulomb breakup could be treated by time dependent perturbation theory at large impact parameters, while it could be described by an all order eikonal model at small impact parameters. Sections III contains results for  $^8\text{B}$ , while Section IV is devoted to  $^{17}\text{F}$ . In Section V the proton and neutron angular distributions due to Coulomb breakup are shortly described. Finally our conclusions are given in Sec.VI.

## II. FORMALISM

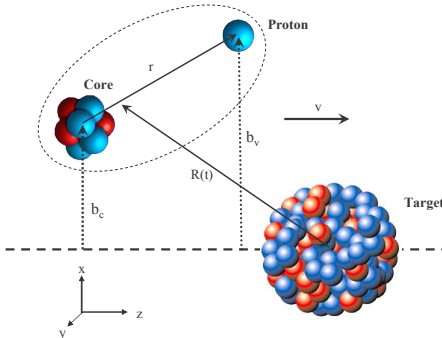


FIG. 1: (Color online). Coordinate system.

The Coulomb potential responsible for proton breakup is

$$V(\vec{r}, \vec{R}) = \frac{V_c}{|\vec{R} - \beta_1 \vec{r}|} + \frac{V_v}{|\vec{R} + \beta_2 \vec{r}|} - \frac{V_0}{R} \quad (1)$$

where  $V_c = Z_c Z_t e^2$ ,  $V_v = Z_v Z_t e^2$  and  $V_0 = (Z_v + Z_c) Z_t e^2$ .  $\beta_1$  and  $\beta_2$  are the mass ratios of proton and core, respectively, to that of the projectile.  $Z_c$ ,  $Z_t$  and  $Z_v$  are the core, target and proton charge respectively. The coordinate system used in this paper is shown in Fig. 1. Following [14, 15], the perturbation theory phase is defined as  $\chi_{pert} = \frac{1}{\hbar} \int dt e^{i\omega t} V(\vec{r}, t)$ , which calculated explicitly gives

$$\begin{aligned} \chi^p = & \frac{2}{\hbar v} (V_c e^{i\beta_1 \omega z/v} K_0(\omega b_c/v) - V_0 K_0(\omega R_\perp/v) \\ & + V_v e^{-i\beta_2 \omega z/v} K_0(\omega b_v/v)) \end{aligned} \quad (2)$$

with  $b_v = b_c + r_\perp$ ,  $\omega = (\varepsilon_f - \varepsilon_0)/\hbar$  and  $\varepsilon_0$  is the neutron initial bound state energy while  $\varepsilon_f$  is the final neutron-core continuum energy. Since  $V_0 = V_c + V_v$ , Eq. (2) can be written as

$$\chi^p = \chi(\beta_1, V_c) + \chi(-\beta_2, V_v) \quad (3)$$

where each term is given by

$$\chi(\beta, V) = \frac{2V}{\hbar v} \left( e^{i\beta\omega z/v} K_0(\omega b/v) - K_0(\omega R_\perp/v) \right), \quad (4)$$

$\chi(\beta_1, V_c)$  describes the recoil of the core whereas  $\chi(-\beta_2, V_v)$  accounts for the direct proton-target Coulomb interaction. The latter vanishes in the case of the neutron.

The expansion of Eq. (4) to first order in  $\vec{r}$  yields the dipole approximation to the phase:

$$\begin{aligned} \chi^p \simeq & \frac{2(\beta_1 V_c - \beta_2 V_v)}{\hbar v} (K_0(\omega R_\perp/v) \frac{i\omega z}{v} \\ & + K_1(\omega R_\perp/v) \frac{\vec{R}_\perp \cdot \vec{r} \omega}{R_\perp v}), \end{aligned} \quad (5)$$

The constant factor is now  $(V_c \beta_1 - V_v \beta_2)$  while for a neutron would be  $V_0 \beta_1$  [15].

We recall here that in Ref.[13] it was suggested that proton breakup could be treated as neutron breakup and the Coulomb potential of Eq.(1) could be approximated by a dipole expansion if the neutron was given an effective binding energy which would take into account the combined effect of the core and target Coulomb barriers. As we mention in the Introduction, this model has been applied in Ref.[1]. Liang et al. used first-order perturbation theory to calculate proton breakup via an increase of the effective binding energy of the valence proton treated as if it were a neutron. The authors fitted their the angular distributions using an increase in the binding energy of 1.2 MeV. We shall show in the following that accurate calculations of proton vs neutron breakup suggest indeed that in certain cases proton breakup can be understood in terms of a more bound neutron breakup. However we believe now that a better estimate of the effective energy is given by

$$\tilde{\varepsilon}_i = \varepsilon_i - \Delta = \varepsilon_i - \frac{Z_p e^2}{R_i} - Z_t e^2 \left( \frac{1}{2} \left( \frac{1}{|d + \beta_2 R_i|} + \frac{1}{|d - \beta_1 R_i|} \right) - \frac{1}{d} \right), \quad (6)$$

which through the factors  $\beta_1$  and  $\beta_2$  is consistent with Eq.(1).  $R_i$  the position of the projectile top of the Coulomb barrier,  $d$  is the distance between the center of the two nuclei for which the top of the two Coulomb barriers of projectile and target coincide.

Our expression for the differential cross-section is

$$\frac{d\sigma}{d\vec{k}} = \frac{1}{8\pi^3} \int d\vec{r}_c |S_{ct}(b_c)|^2 |g^{rec} + g^{dir} + g^{nuc}|^2. \quad (7)$$

where  $|S_{ct}(b_c)|^2$  is the core-target elastic scattering probability.

The probability amplitude in Eq.(7) has been written as the sum of three pieces: the recoil term,

$$\begin{aligned} g^{rec} = & \int d\vec{r} e^{-i\vec{k} \cdot \vec{r}} \phi_i(\vec{r}) (e^{i\frac{2V_c}{\hbar v} \log \frac{b_c}{R_\perp}} - 1 - i \frac{2V_c}{\hbar v} \log \frac{b_c}{R_\perp} \\ & + i\chi(\beta_1, V_c)), \end{aligned} \quad (8)$$

obtained in the sudden limit according to [14, 15] in order to include all orders in the final state Coulomb interaction of the core with the target. Similarly, the second term in our probability amplitude is the direct proton Coulomb interaction. It has the same form as Eq.(8) but for the substitution  $V_c \rightarrow V_v$ ,  $b_c \rightarrow b_v$  and  $\beta_1 \rightarrow -\beta_2$ . Both the direct and recoil term contain a regularization of the first order term divergency consisting in substituting it with the corresponding first order perturbation theory term. Such regularization method was first proposed in Ref.[20] and used also in Refs.[21, 22].

Finally, the nuclear part is

$$g^{nuc} = \int d\vec{r} e^{-i\vec{k} \cdot \vec{r}} \phi_i(\vec{r}) (e^{i\chi_{nt}(b_v)} - 1). \quad (9)$$

If the Coulomb part of the amplitude  $g^{Coul} = g^{rec} + g^{dir}$  is simply expanded to first order in  $\chi$  and it is written, in terms of the one-dimensional Fourier transform in  $z$ -direction  $\hat{\phi}_i$ , then making also the dipole approximation one gets:

$$g^{Coul} \simeq \int d\vec{r}_\perp e^{-i\vec{k}_\perp \cdot \vec{r}_\perp} \frac{2(\beta_1 V_c - \beta_2 V_v)}{\hbar v} \times \left( K_0(\omega R_\perp/v) \frac{\omega}{v} \frac{d}{dk_z} \hat{\phi}_i(\vec{r}_\perp, k_z) + K_1(\omega R_\perp/v) \frac{\vec{R}_\perp \cdot \vec{r}}{R_\perp} \frac{\omega}{v} \hat{\phi}_i(\vec{r}_\perp, k_z) \right), \quad (10)$$

leading to symmetric momentum distributions.

A number of experimental data for neutron breakup have been analyzed by separating high impact parameters such that perturbation theory would be valid. We shall try in the following to do the same for proton breakup and in order to clarify the effects of the Coulomb interaction we will show separately results for the Coulomb or nuclear probability only. Furthermore we will show momentum probability distributions at fixed impact parameters, namely:

$$\frac{dP(b_c)}{dk_z} = \frac{1}{8\pi^3} \int d\vec{k}_\perp |g(b_c)|^2. \quad (11)$$

$|g(b_c)|^2$  will be the nuclear or Coulomb amplitude and in the latter case we will indicate in which approximation the calculation was done.

### III. APPLICATION TO ${}^8\text{B}$

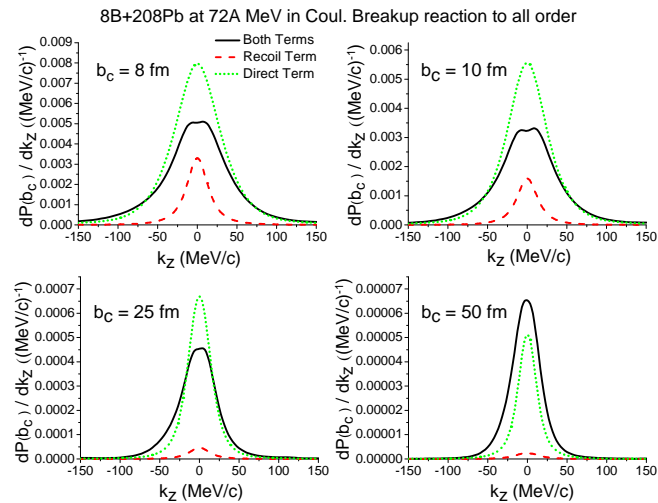


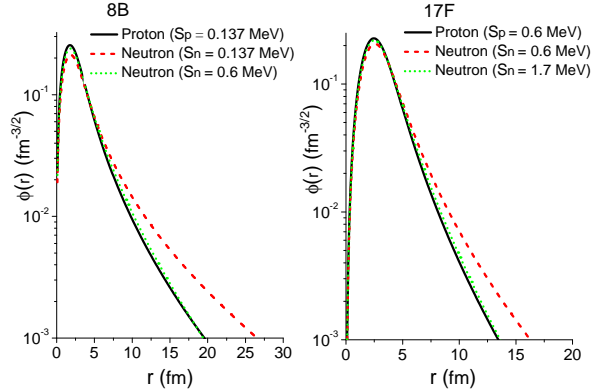
FIG. 2: (Color online). Recoil term, Eq. (8), red dashed line and direct term, green dotted line. The black full line contains both.

In our previous work in which the method presented here was introduced, we applied it to study a reaction at 936A.MeV, the energy was high enough to justify the eikonal approximation. Before starting the calculations presented in this and the following section we have compared our results for the total breakup probabilities against the values provided by Ref.[18]. We have found that for nuclear breakup our results agree with the dynamical calculations down to 10A.MeV if we substitute the impact parameter by the distance of closest approach of the corresponding classical trajectory. For Coulomb breakup our probabilities decrease with the impact parameter as those of Ref.[18] but they are about 50% larger. This is due to the use of a straight line relative motion trajectory in our method. For nuclear

TABLE I: Barrier radii, initial binding energies and effective energy parameters for a  $^{208}\text{Pb}$  target.

	$^8\text{B}$	$J^\pi$	$^{17}\text{F}$	$J^\pi$
$R_i(\text{fm})$	6.0		6.5	
$\varepsilon_i(\text{MeV})$	-0.14	$1\text{p}_{3/2}$	-0.6	$1\text{d}_{5/2}$
$\varepsilon_i^*(\text{MeV})$	-0.57	$1\text{p}_{1/2}$	-0.1	$2\text{s}_{1/2}$
$-\Delta(\text{MeV})$	-0.4		-1.2	
$\tilde{\varepsilon}_i(\text{MeV})$	-0.54	$1\text{p}_{3/2}$	-1.8	$1\text{d}_{5/2}$
$\tilde{\varepsilon}_i^*(\text{MeV})$	-0.97	$1\text{p}_{1/2}$	-1.3	$2\text{s}_{1/2}$

breakup the substitution of the impact parameter with the distance of closest approach is enough to cure the method, because the nuclear form factors are different from zero only in a small region around the distance of closest approach where the classical trajectory is well approximated by a straight line. On the other hand the same cannot be said of the Coulomb form factor. We have checked however that our method starts to give reliable absolute probability values around 70-100A.MeV which agrees with what we found in our previous works on neutron breakup [19, 20].

FIG. 3: (Color online). Proton vs neutron wave functions for a  $p_{3/2}$  single particle state in a  $^8\text{B}$  and  $^{17}\text{F}$  as indicated.

Thus the formalism described in the previous section has been applied to proton breakup of  $^8\text{B}$  and  $^{17}\text{F}$  against  $\text{Pb}$  target at a beam energy of 72A.MeV which is a typical energy used in several laboratories and for which our results should be reliable. The projectiles are taken as a two-body object. Radial wave functions have been obtained by numerical solution of the Schrödinger equation in Woods-Saxon potentials with depths adjusted to reproduce the experimental separation energies (0.137MeV and 0.6MeV respectively). The radius parameter of these Woods-Saxon potentials has been taken as 1.3 fm and the diffuseness as 0.6 fm.

In Fig.2 we show separately the effect of the recoil, Eq. (8) term, red dashed line while the green dotted line represents the direct term obtained from  $g^{dir}$ . The black full line contains both. It is clear that the interference between the two is mostly destructive and it becomes constructive only at very large impact parameters. This effect is the equivalent in our model of what Liang et al. [1] call the "shielding effect" of the proton by the core. The direct term alone, being proportional to  $\beta_2$  is indeed in absolute value always larger than the recoil term. However it is the effect of the interference between direct and recoil terms that causes the reduction of the Coulomb breakup in the proton halo case.

Following Refs.[1] and [13] we have then calculated the Coulomb breakup to all orders (regularized) and in the dipole approximation for a neutron with several different binding energies. Our hypothesis, that one could use a neutron wave function corresponding to an *effective* separation energy  $S_n$  larger than that of the proton, has been checked for various values of  $S_n$  and we have found that for  $S_n = 0.6$  MeV the model works quite well. This is a factor four smaller than the value  $S_n = 2.4$  MeV predicted in [13]. Liang et al. in [1] found indeed that in the description of the breakup of  $^{17}\text{F}$  the dipole approximation and perturbation theory to first order could be used by introducing a neutron wave function corresponding to an effective energy smaller by about a factor three than the one of our

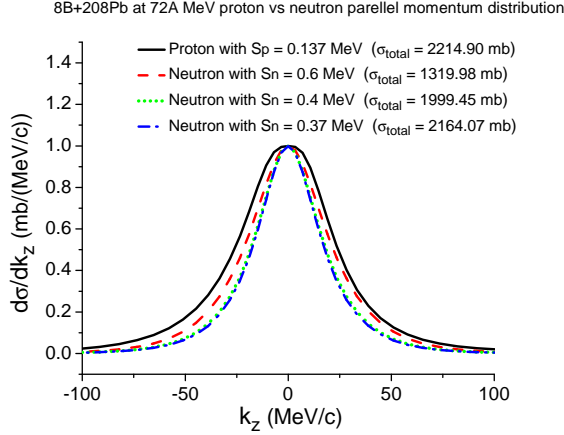


FIG. 4: (Color online). Differential cross sections for neutrons of different separation energies and proton breakup cross section, all normalized to one. The integrated values are given in the legend.

original model. The reason is that the model of [13] used an effective binding energy given by an intuitive but not very accurate expression. In this work we use instead Eq.(6) which through the factors  $\beta_1$  and  $\beta_2$  is more consistent with the Coulomb potential definition. In order to understand the proton vs neutron breakup dynamics we start by showing in Fig.3 LHS the single particle wave function ( $S_p = 0.137$  MeV) for a  $p_{3/2}$  proton with respect to a  $^7\text{Be}$  core by the full black line, for a neutron with the same  $S_n$  by the red dashed line and finally for a neutron with  $S_n = 0.6$  MeV by the green dotted line. The RHS is for  $^{17}\text{F}$  wave function.

We have made all order proton calculations and calculations for a neutron of separation energy  $S_n = 0.137$  MeV and  $S_n = 0.6$  MeV. In the latter case we have studied the impact parameter dependence of the momentum distributions obtained to all order and compared the results to those corresponding to the dipole approximation. It is interesting to note that as discussed in [13], and in particular in the appendix of that work, the dipole approximation for a neutron of large binding energy reproduces quite well the proton exact calculation and becomes actually identical to it at large impact parameters.

At this stage we remind the reader that in the case of breakup of a neutron both the "small" width of the momentum distribution and large breakup cross sections were due to the small separation energy and corresponding long tail of the wave function. The proton breakup characteristics are instead quite different as we can interfere from Fig.4. It shows the proton breakup parallel momentum distribution from  $^8\text{B}$  on a  $^{208}\text{Pb}$  target compared to three distributions from an hypothetical neutron bound by three possible energies as indicated. The distributions are normalized to one. The total breakup cross sections including nuclear and Coulomb interactions to all orders are given in the legend. The smallest neutron separation energy case provides the closest cross section to the proton's one while it is in the largest separation energy case that the neutron distribution width gets closest to the proton distribution width. This is consistent with the fact that it is the tail of neutron wave function corresponding to  $S_n = 0.6$  MeV in Fig.3 which is closest to the proton's wave function tail.

Therefore we understand that as in the neutron case, the large cross sections are associated with small separation energy but the corresponding momentum distributions have large width because the wave functions do not have an extended tail. The model of a neutron of larger separation energy representing a proton of smaller separation energy works therefore well for nuclear breakup. In the case of the proton Coulomb breakup the results are not easy to interpret instead because direct and recoil terms interfere mostly destructively (cf. Fig(2)). However the interference becomes constructive at the very large impact parameters where the recoil term is negligible. There, a large breakup can be seen as a consequence of the direct term which as Eq.(5) shows, being proportional in first order to  $\beta_2$ , will be large if the proton is well displaced from the core.

We have also studied the spectra corresponding to the  $m=0,1$  components of the wave function for the direct and recoil terms in Coulomb breakup including interference and we compared to the same quantities in the case of a neutron. The  $m=0$  component gives asymmetric distributions while the  $m=1$  component gives symmetric distributions. These results indicate that small polarization effects can lead to asymmetric spectra in the proton case and that this is due to the large direct breakup term. Neutron spectra do not show this effects.

#### IV. APPLICATION TO $^{17}\text{F}$

We start this section by suggesting the reader to look at the proton wave function for the  $d_{5/2}$  ground state of  $^{17}\text{F}$  back in Fig. 3. The same figure contains two neutron wave functions for separation energies as indicated that we have used in the calculations shown in the subsequent Figs.5, 6 and 7.

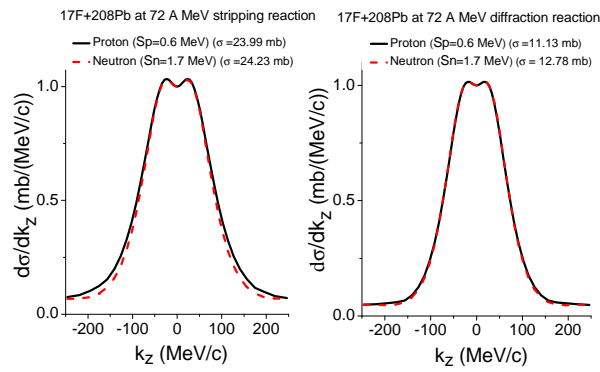


FIG. 5: (Color online). Diffraction and stripping terms of the nuclear breakup of the proton  $d_{5/2}$  ground state in  $^{17}\text{F}$

By looking at the wave functions in Fig. 3 and the nuclear breakup diffraction and stripping terms, Fig.5 we see that the "neutron-like" model works well also for the  $d_{5/2}$  ground state in  $^{17}\text{F}$  at 72 A.MeV incident energy. The best "model" separation energy here seems to be 1.7MeV. This value is larger than what suggested in [1] but smaller than the value predicted in [13]. It agrees well with our new effective energy estimate Eq.(6).

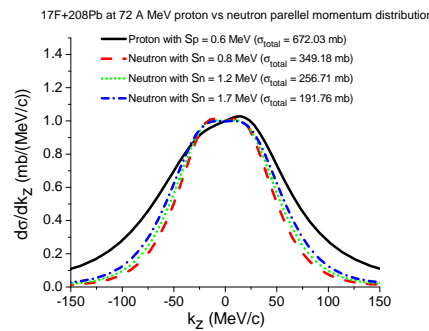


FIG. 6: (Color online). Differential breakup cross sections for neutrons of different separation energies and the proton ( $d_{5/2}$  ground state in  $^{17}\text{F}$ ) cross section. All normalized to one. The integrated values are given in the legend.

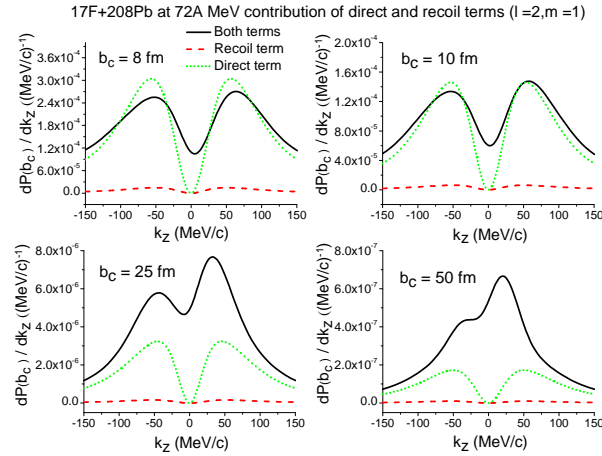


FIG. 7: (Color online). Direct and recoil terms in Coulomb breakup for the  $m=1$  component of the  $^{17}\text{F}$  wave function.

To finish this section we show in Fig.6 the total cross section distribution for the breakup of the  $d_{5/2}$  proton ground state in  $^{17}\text{F}$  at 72 A.MeV, compared to two neutron breakup distributions. What is evident here is a strong asymmetry in the spectrum which instead does not appear in the neutron case. Also in this case the presence of a direct Coulomb breakup term is extremely important because the recoil term is strongly reduced by the centrifugal barrier of the  $d$ -state. The immediate consequence is that now the interference between direct and recoil term is mostly constructive. The asymmetry in the spectrum originates from the interference of direct and recoil term which is present in the low ( $m=0,1$ ) components of the initial wave function which dominate the breakup spectrum. Such effects are shown by Fig. 7 which contains the probability spectra for the  $m=1$  projection of the initial angular momentum wave function. The  $m=2$  component gives a symmetrical distribution not shown here.

## V. ANGULAR DISTRIBUTIONS

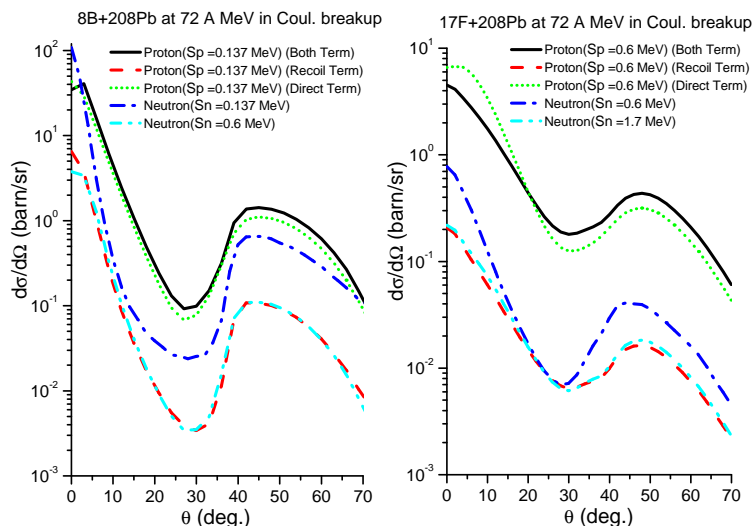


FIG. 8: (Color online). Proton and neutron angular distributions after breakup. Details are given in the legend.

This section is devoted to the discussion of the angular distributions of the breakup protons presented in Fig.8. Here again we show the total result for protons and at the same time the direct and recoil terms. We show also two calculations for neutrons. One for neutron having the same binding energy as the proton and the other for the effective energy previously obtained. It is very interesting to see that the recoil term of the proton calculation and the calculation for a neutron with the effective binding energy give very close results. This confirms the interpretation that the core-target Coulomb effect is basically a recoil effect for which the difference between a neutron and a proton is that the proton looks "more effectively" bound. On the other hand the direct term gives the most important contribution to the proton breakup, its interference with the recoil term is sometimes constructive, sometimes destructive. This term is not present in the neutron case and it is at the origin of the special dynamical effects of proton breakup

Finally we notice that a neutron of the same binding energy as the proton would give quite a large breakup in the case of the p-state of  $^8\text{B}$ , thus suggesting a halo-like behavior for this nucleus, while for  $^{17}\text{F}$  a neutron of the same binding would anyhow give much less breakup at most angles. We can understand this effect by looking at the wave functions in Fig.3. The tail of a neutron wave function for  $^8\text{B}$ , being a p-state, is much more pronounced than the tail of a possible d-neutron wave function in  $^{17}\text{F}$ . Therefore there is no "structural" halo effect in the Fluorine case but the large proton breakup probability in this case has a dynamical origin being due to the strong direct proton-target repulsion.

## VI. CONCLUSIONS

In this paper we have calculated proton and neutron Coulomb and nuclear breakup from  $^8\text{B}$  and  $^{17}\text{F}$  at 72 A.MeV on a  $^{208}\text{Pb}$  target. Our method is an all order formalism based on the eikonal approximation, with a regularized first order Coulomb term. We have compared proton to neutron parallel momentum distributions and angular distributions. The neutron cases have been calculated for an "hypothetical" neutron having the same separation energy and angular momentum as the proton in the two projectiles and compared to calculations for a neutron having an *effective* binding energy larger than the true proton experimental binding energy. The effective values take into account the combined effects of the projectile and target Coulomb barrier. We have given an explicit formula to evaluate the effective energy which is in agreement with phenomenological findings. The model has been used to understand the origin of the strong dynamical effects seen in Coulomb breakup data. Our results clearly show that as far as the nuclear breakup mechanism is concerned the proton behaves as a neutron of larger separation energy. On the other hand parallel momentum distributions are affected by the recoil due to the neutron-core Coulomb potential and by the direct repulsion due to proton-target Coulomb potential, in a complicated way. This happens both in the calculations, as well as in the data. There are interference effects between the direct and recoil term which depend on the impact parameter. Thus even if they can be understood in the theoretical calculation, they would be difficult to disentangle in an experiment. Effects on the core angular distributions are also complicated and will be discussed in a forthcoming publication. However we have finally shown that the proton angular distributions would be a very good observable to study experimentally in order to separate the two Coulomb effects. Our results indicate that the proton angular distributions are dominated by the direct term while the recoil term gives almost an order of magnitude smaller cross section as a function of the proton angle. A neutron of the appropriate *effective* binding energy would have exactly the same angular distribution as that given by the recoil term for the proton. On the proton angular distributions the effects of interference seem to be negligible and we have found some only in the very forward angle region for the  $^{17}\text{F}$  projectile. We have also concluded that a large breakup cross section for a weakly bound proton can originate from dynamical effects without corresponding to an unusual structure of the bound state. Thus we have clarified the way in which the Coulomb barrier affects weakly bound protons in exotic proton rich nuclei off the stability line. We hope that our results would give some guideline not only in planning future breakup experiments for spectroscopic and astrophysical studies but more in general in studying the interplay between structure and dynamics of nuclei with weakly bound protons.

---

[1] J.F. Liang, J.R. Beene, A.L. Caraley, H. Esbensen, A. Galindo-Uribarri, C.J. Gross, P.E. Mueller, K.T. Schmitt, D. Shapira, D.W. Stracener, R.L. Varner, Phys. Lett. **B681** 22 (2009).  
[2] G. Baur, C.A. Bertulani, H. Rebel, Nucl. Phys. **A458** 188 (1986).  
[3] T. Motobayashi, et al., Phys. Rev. Lett. **73** 2680 (1994).  
[4] T. Kikuchi, et al., Phys. Lett. **B391** 261 (1997).  
[5] B. Davids, et al., Phys. Rev. C **63** 065806 (2001).  
[6] H. Esbensen, G.F. Bertsch, C.A. Bertulani, Nucl. Phys. **A581** 107 (1995).  
[7] T. Nakamura, et al., Phys. Rev. C **79** 035805 (2009).

- [8] H. Esbensen, G.F. Bertsch, Phys. Rev. C **66** 044609 (2002).
- [9] H. Esbensen, G.F. Bertsch, K.A. Snover, Phys. Rev. Lett. **94** 042502 (2005).
- [10] A. Deltuva, A. C. Fonseca, and P. U. Sauer, Phys. Rev. Lett. **95** 092301 (2005).
- [11] R. Crespo, M. Rodriguez-Gallardo, A. M. Moro, A. Deltuva, E. Cravo, and A. C. Fonseca Phys. Rev. C 83, 054613 (2011) and references therein.
- [12] Report on the Second EURISOL Topical Meeting, Valencia, 21-24 February 2011, Ed. B. Rubio, B. Blank, L. Ferreira and A. Bonaccorso, in preparation, to appear on [www.eurisol.org/usergroup](http://www.eurisol.org/usergroup).
- [13] A. Bonaccorso, D. M. Brink and C. A. Bertulani, Phys. Rev. C **69** 024615 (2004).
- [14] A. García-Camacho, G. Blanchon, A. Bonaccorso and D. M. Brink, Phys. Rev. C **76** 014607 (2007).
- [15] A. García-Camacho, A. Bonaccorso and D. M. Brink, Nucl. Phys. **A776** 118 (2006).
- [16] L. Lo Monaco and D. M. Brink, J.Phys. G **11** (1985) 935.
- [17] A. Bonaccorso, D. M. Brink, Phys. Rev. C **38** (1988) 1776.
- [18] H. Esbensen, G. F. Bertsch, Nucl. Phys. **A706** 383 (2002).
- [19] J. Margueron, A. Bonaccorso and D. M. Brink, Nucl. Phys. **A703** 105 (2002).
- [20] J. Margueron, A. Bonaccorso and D. M. Brink, Nucl. Phys. **A720** 337 (2003).
- [21] B. Abu-Ibrahim and Y. Suzuki, Prog. Theor. Phys. 112, 1013 (2004); 114, 901 (2005).
- [22] P. Capel and D. Baye and Y. Suzuki, Phys. Rev. C **78** (2008) 054602.